Title

Imaging of Conductivity Distributions Using Audio-Frequency Electromagnetic Data

Authors
Lee, K H
Morrison, H F

Publication Date
1990-10-01

LBL-30081

Lawrence Berkeley Laboratory
UNIVERSITY OF CALIFORNIA

EARTH SCIENCES DIVISION

To be presented at the International Symposium
on Geotomography, Tokyo, Japan, December 10–11, 1990,
and to be published in the Proceedings

Imaging of Conductivity Distributions Using Audio-Frequency Electromagnetic Data

K.H. Lee and H.F. Morrison

October 1990

Prepared for the U.S. Department of Energy under Contract Number DE-AC03-76SF00098.

LBL-30081

Imaging of Conductivity Distributions Using Audio-Frequency Electromagnetic Data

Ki Ha Lee

Earth Sciences Division
Lawrence Berkeley Laboratory
University of California
Berkeley, California 94720

and

H. Frank Morrison

Department of Materials Science and Mineral Engineering
University of California
Berkeley, California 94720

October 1990

This work was supported by the Director, Office of Energy Research, Office of Basic Energy Sciences, Engineering and Geosciences Division, of the U.S. Department of Energy under Contract No. DE-AC03-76SF00098.

Imaging of Conductivity Distributions Using Audio-Frequency Electromagnetic Data

Ki Ha Lee (Earth Sciences Division, Lawrence Berkeley Laboratory, Berkeley, CA. 94720, USA)
H. Frank Morrison (Department of Materials Science and Mineral Engineering, University of California, Berkeley, CA. 94720, USA)

Summary

The objective of this study has been to develop mathematical methods for mapping conductivity distributions between boreholes using low frequency electromagnetic (em) data. In relation to this objective this paper presents two recent developments in high-resolution crosshole em imaging techniques. These are (1) audio-frequency diffusion tomography, and (2) a transform method in which low frequency data is first transformed into a wave-like field. The idea in the second approach is that we can then treat the transformed field using conventional techniques designed for wave field analysis.

The audio-frequency imaging technique is new and has been developed for fracture detection, reservoir description, and ground water monitoring. The frequency range used for this application is from essentially dc to 100 kHz. Unlike high-frequency radar systems with applications mostly in shallow reflection surveys, an audio-frequency em tool would be useful for achieving deeper penetrations. Laboratory experiments show that the seismic velocity does not change significantly until the rock is fully saturated. The electrical conductivity in unsaturated rocks, however, increases dramatically as the saturation is increased. At higher saturation, after most of the individual pore spaces are fully connected by fluids, the increase in conductivity slows down. In this respect a joint application of seismic and em methods can be highly complementary in characterizing geomechanical, and ultimately geohydrological properties of rocks.

For the development and subsequent verification of imaging techniques to be efficient it is critically important that high quality em data is readily available. However, the effort involved in developing high precision instruments and state-of-art field techniques for carrying out a survey on a realistic field scale is prohibitive. For this reason we have been conducting a scale-model em experiment at the Richmond Field Station (RFS), University of California, Berkeley. Our initial data from the experiment show excellent agreements with numerical solutions.

Diffusion tomography

A tomographic inversion scheme has been developed (Zhou, 1989) for interpreting audio-frequency em data. The formulation of this new approach, called diffusion tomography, is related to the recent developments in acoustic diffraction tomography (Devaney, 1982; Wu and Toksoz, 1987). There exists, however, a significant mathematical difference in that the background wave number in the acoustic case is real while that in the em case is complex. By extending the acoustic image reconstruction formulation through the introduction of an inverse Laplace transform in place of the inverse Fourier transform, the method can now be applied to map electrical conductivity distributions between boreholes. Although the algorithm development is based on the traditional Born or Rytov weak scattering approximation, it has been found later that the technique is surprisingly effective even when the conductivity anomaly is strong. The approach was first investigated using two-dimensional (2-D) models. Following this simple but useful model studies, more complex and realistic structures with a cylindrical symmetry and 3-D problems have been examined. The results from these last two cases have been found to be similar to that of the 2-D case if a geometrical correction factor is applied to the data.

The 2-D diffusion tomography algorithm is based on the integral equation for the electric field

$$E^s(r_r, r_s) = \int_S \Delta\sigma \, E(r, r_s) \, G(r, r_r) \, dxdz \qquad (1)$$

where the superscript 's' indicates the secondary field. In this development we assume that the source is located in one borehole (r_s) and the receiver in the other (r_r). Applying the Born approximation by which the electric field inside the integral is replaced by the primary field, and Fourier transforming both sides of the resulting equation from r_r and r_s to k_r and k_s, respectively, equation (1) becomes

$$\widetilde{E}^s(k_r, k_s) \, W(\gamma_r, \gamma_s) = \int_S O(r) \exp(-s_x x - i k_z z) \, dxdz \qquad (2)$$

where the object function O(r) is defined as the conductivity ratio of the anomalous to the background. The weight function W in this expression is essentially identical to the one used for the diffraction tomography (Wu and Toksoz, 1987). Note that a Laplace variable s_x is used instead of the spatial wave number k_x (Zhou, 1989). By inspection the solution for the object function can be formally written as

$$O(r) = \frac{1}{(2\pi)^2 i} \int ds_x \int \widetilde{E}^s(k_r, k_s)\, W(\gamma_r, \gamma_s) \exp(s_x x + i k_z z)\, dk_z \qquad (3)$$

The above operation involves inverse Fourier transform from k_z to z, and inverse Laplace transform from s_x to x. It is well known, however, that the numerical inverse Laplace transform is unstable. To ensure the stability of the numerical solution one needs to apply constraints to the solution process as required by regularization theory for ill-posed problems in general. If we assume that the zone of interest is electrically more conductive than the background, for example, the object function has to positive. We can incorporate this positivity constraint by first discretizing the integral equation (2), and then solving the resulting constrained least squares or a quadratic programming problem. In addition to constraints for stability a smoothing step may also be necessary. Any sharp variations in the numerical solution is usually artificial and algorithm dependent, since in most cases high spatial wave number information is absent and the noise can be easily amplified in the repeated numerical process.

Figure 1-(a) shows a sample model representing a cylindrically symmetric conductive plume as a result of an injection experiment. The conductivity of the plume is 0.02 S/m. This is only slightly more conductive than the background conductivity of 0.01 S/m. The question in this exercise has been; can we, at least in principle, use the diffusion tomography to monitor the laterally expanding plume as injection is continued? Based on the result of our numerical test, it seems that the answer to this question is positive. Using computer simulated data in a crosshole environment, the image of the expanding plume has been successfully constructed as shown in Figures 1-(b), 1-(c), and 1-(d) corresponding to Lx = 20m, 40m, and 60m, respectively.

To provide data for testing numerical algorithms an em scale model study has been conducted at the Richmond Field Station (RFS), University of California, Berkeley. The scale model consists of a container of size 9'x15'x5' filled with salt water of approximately 14 S/m. Graphite blocks are used as targets and an array of transmitter and receiver coils are used to measure the resulting magnetic fields. The system has been designed such that data is collected at a fixed position while the transmitter is moved continuously. This provides for both low noise measurements and relatively quick acquisition.

Wave-field transform method

There have been several studies in the past implying that there is an interesting parallelism between the mathematical form for the em diffusion equation and the wave equation (Weidelt, 1972; Kunetz, 1972; and Levy et al., 1988). The subject of these studies has been essentially limited to the magnetotelluric (MT) method in a layered (1-D) medium.

For practical situations, typically involving a multi-dimensional space and an arbitrary source, Lee et al. (1989) have presented a more fundamental relationship between fields satisfying a diffusion and the corresponding wave equations. The relationship is defined by an integral transform that is completely independent of space variables. In this relationship the diffusive field, the electric field **E** for example, is uniquely represented by an integral of a corresponding wave field **U** weighted by an exponentially damped kernel. This fictitious field **U** would be dispersionless and would have a well defined phase, as well as a group, velocity. It has been shown that, as an application, the transform can be used for numerical modeling of em fields. In this application the wave field is first computed numerically, and then the em field is subsequently calculated using the integral. More importantly, it was also suggested (Lee, 1987) that an inverse transform could be used to transform field data measured in time (or in frequency) to the wave field in a time-like variable q. The inverse transform requires that the data be of wideband to yield waveforms of reasonable resolution. The other important factor that determines the resolution of the constructed wave field is the level of estimated noise contained in the data. For stability reasons a stochastic approach has been used to construct the wave field. Thus constructed wave field could then be used for further analysis for conductivity mapping using migration techniques, or even more sophisticated wave equation imaging or tomographic reconstruction techniques.

The following is a brief description of the study by Lee et al. (1989) concerning the formal relationship between quantities satisfying the diffusion and the wave equations. In the presence of a current source, **S**(**r**,t), the electric field satisfies the vector diffusion equation in 3-D

$$\nabla\times\nabla\times\mathbf{E}(\mathbf{r},t) + \mu\sigma(\mathbf{r})\frac{\partial}{\partial t}\mathbf{E}(\mathbf{r},t) = \mathbf{S}(\mathbf{r},t) \qquad (4)$$

With the introduction of functions **U**(**r**,q) and **F**(**r**,q), such that

$$\nabla\times\nabla\times\mathbf{U}(\mathbf{r},q) + \mu\sigma(\mathbf{r})\frac{\partial^2}{\partial q^2}\mathbf{U}(\mathbf{r},q) = \mathbf{F}(\mathbf{r},q), \qquad (5)$$

It has been shown that the diffusive electric field **E** in equation (4) and the wave field **U** in equation (5) are uniquely related by

$$\mathbf{E}(t) = \frac{1}{2\sqrt{\pi t^3}}\int_0^\infty q\, e^{-\frac{q^2}{4t}}\,\mathbf{U}(q)\,dq. \qquad (6)$$

The wave equation (5) implies that each components of the wave field **U** would have a velocity of $(\mu\sigma)^{-1/2}$ m/q. The position vector **r** has been dropped from the expression since the transformation is independent from it.

As an initial step to imaging conductivity distributions it was suggested that we first solve this integral equation for the wave field **U**(q) from the data **E**(t). In what follows we will briefly discuss a closed form solution, among other potentially useful methods, presented by Lee (1987). First, both sides of equation (6) are Fourier transformed (from t to ω) to yield

$$\tilde{\mathbf{E}}(\omega) = \int_0^\infty e^{-\sqrt{i\omega}q}\,\mathbf{U}(q)\,dq. \qquad (7)$$

Taking only the imaginary part, for example, of this equation and applying change of variables

$$\omega = 2e^{2u}, \qquad q = e^{-v}$$

with following definitions

$$\mathbf{D}(u) = e^{u}\,\mathrm{Im}\{\tilde{\mathbf{E}}(2e^{2u})\}, \quad H(u) = e^{-e^{u}}\sin(e^{u})\,e^{u}, \quad \mathbf{W}(v) = \mathbf{U}(e^{-v})$$

it can be shown that solution for **W** is found to be

$$\mathbf{W}(v) = -\frac{1}{2\pi}\int_{-\infty}^{\infty}\frac{\tilde{\mathbf{D}}(\eta)}{\tilde{H}(\eta)}\,e^{i\eta v}\,d\eta, \qquad (8)$$

where $\tilde{\mathbf{D}}(\eta)$ and $\tilde{H}(\eta)$ are again Fourier transform (from u to η) of functions **D**(u) and H(u), respectively.

Although the solution given by equation (8) is analytically in a closed form, it is extremely unstable to evaluate numerically. The deconvolution kernel $\widetilde{H}(\eta)$ is exponentially damped in η, and as a result, distributed noise, especially those in higher spectrum, contained in the data $\widetilde{D}(\eta)$ will be exponentially amplified. This is well expected since the original linear inverse problem for the wave field **U** in equation (6) is ill-posed. A practically useful solution would involve a stochastic approach (Franklin, 1970; Aki and Richards, 1980), for which we may need an estimated noise to the problem. If the noise is statistically unrelated to the model (wave field), the solution for the modified equation is simply

$$\mathbf{W}^*(v) = -\frac{1}{2\pi}\int_{-\infty}^{\infty} \widetilde{G}(\eta)\,\frac{\widetilde{\mathbf{D}}^*(\eta)}{\widetilde{H}(\eta)}\,e^{i\eta v}\,d\eta, \tag{9}$$

with its optimum inverse filter $\widetilde{G}(\eta)$ given by

$$\widetilde{G}(\eta) = \frac{|\widetilde{H}(\eta)|^2}{\dfrac{\sigma_N(\eta)}{\sigma_W(\eta)} + |\widetilde{H}(\eta)|^2}\,. \tag{10}$$

Here $\sigma_N(\eta)$ and $\sigma_W(\eta)$ are estimated power spectrum of noise and signal, respectively. When there is no noise equation (9) would be identical to equation (8). However, if the noise increases in η the deconvolution integral would become a low pass operation. The inverse filter forces the deconvolution integral stable by effectively cutting off those harmonic contributions from below the specified noise level. This feature is in fact similar to that of the generalized inverse scheme, in which contributions associated with those eigenvalues below a threshold are selectively eliminated at the expense of reduced resolutions. The impulse response of G(v) can therefore be considered the upper limit of the resolution for the constructed wave field.

A numerical test has been made using a model shown in Figure 2. The model consists of a circular cylinder in a whole space of conductivity 0.01 S/m. The cylinder is a 0.5 S/m conductor with a radius of 100 m. A line source is located at 200 m to the left of the center of the cylinder, and the voltage induced in a vertical coil is computed at positions along the receiving borehole 200 m to the right of the center of the cylinder. The computed frequency-domain voltage corresponds to the line source whose current has been abruptly turned off. A wideband frequency response has been used to construct wave fields in the receiving borehole. The simulated wave fields are shown in Figure 3 at every 20 m intervals. An inverse filter with an estimated noise level of three percent has been used for this exercise. By inspection one can now visualize the wave field propagate from the source to each receiver positions. For example, at the first receiver position opposite to the source, the first arrival seems to be made up of waves that propagate around the cylinder with the higher velocity of the surrounding medium. After a pronounced delay, the direct wave transmitted through the conductor arrives at this position with its amplitude much larger than the first arrival. As the receiver is moved down the effect of the diffraction by the cylinder gradually disappears, and the higher-velocity direct wave starts dominating.

The wave field reconstruction from the integral equation is still at its early stage. The most difficult problem in this approach is in finding ways to reduce the amount of data required for constructing wave fields without losing resolutions. Solutions for the wave field can also be obtained numerically from integral equations (6) and (7), depending upon the type of data available. The fundamental difficulty stemming from the ill-posedness of the original problem would remain no matter what we do. It is therefore a question of finding optimum constraints to individual problems and properly applying them to each solution process.

References

Aki, K. and Richards, P. G., 1980, Quantitative Seismology: Theory and Methods: W. H. Freeman and Company, San Francisco, California.

Devaney, A. T., 1982, A filtered back propagation algorithm for diffraction tomography: Ultrasonic Imag., 4, 336-350.

Franklin, J. N., 1970, Well-posed stochastic extension of ill-posed linear problems: Jour. of Math. Anal. and Appl., 31, 682-716.

Kunetz, G., 1972, Processing and interpretation of magnetotelluric soundings: Geophysics, 37, 1005-1021.

Lee, K. H., 1987, A new approach to modeling and interpreting electromagnetic sounding data: Lawrence Berkeley Laboratory Report LBL-23544.

Lee, K. H., Guimin, L., and Morrison, H. F., 1989, A new approach to modeling the electromagnetic response of conductive media: Geophysics, 54, 1180-1192.

Levy, S., Oldenburg, D., and Wang, J., 1988, Subsurface imaging using magnetotelluric data: Geophysics, 53, 104-117.

Weidelt, P., 1972, The inverse problem of geomagnetic induction: Zeit. fur Geophys., 38, 257-298.
Wu, R. S. and Toksoz, M. N., 1987, Diffraction tomography and multisource holography applied to seismic imaging: Geophysics, 52, 11-25.
Zhou, C., 1989, Audio-frequency Electromagnetic tomography for reservoir evaluation: Ph.D. thesis, University of California, Berkeley.

Figure caption

Figure 1-(a) Simulated conductive plume with its horizontal extension Lx in meter. The plume is cylindrically symmetric about the injection borehole.

Figure 1-(b) Reconstructed plume with its lateral extension Lx = 20m.

Figure 1-(c) Reconstructed plume with its lateral extension Lx = 40m.

Figure 1-(d) Reconstructed plume with its lateral extension Lx = 60m.

Figure 2 A cylindrical conductor between boreholes with assumed straight ray paths.

Figure 3 Computed total wave fields for a fixed source.

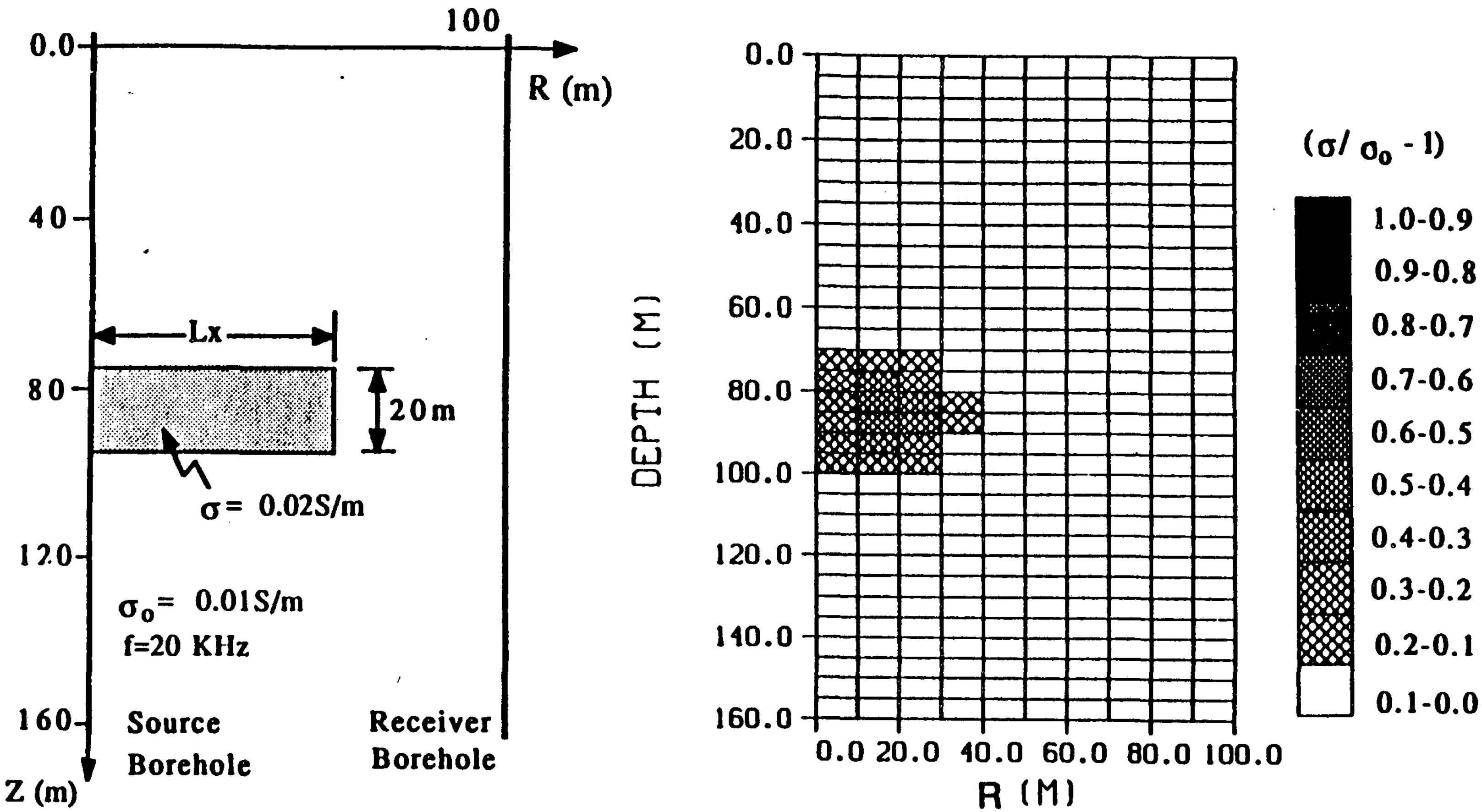

(a) Model

(b) Lx= 20m

Figure 1

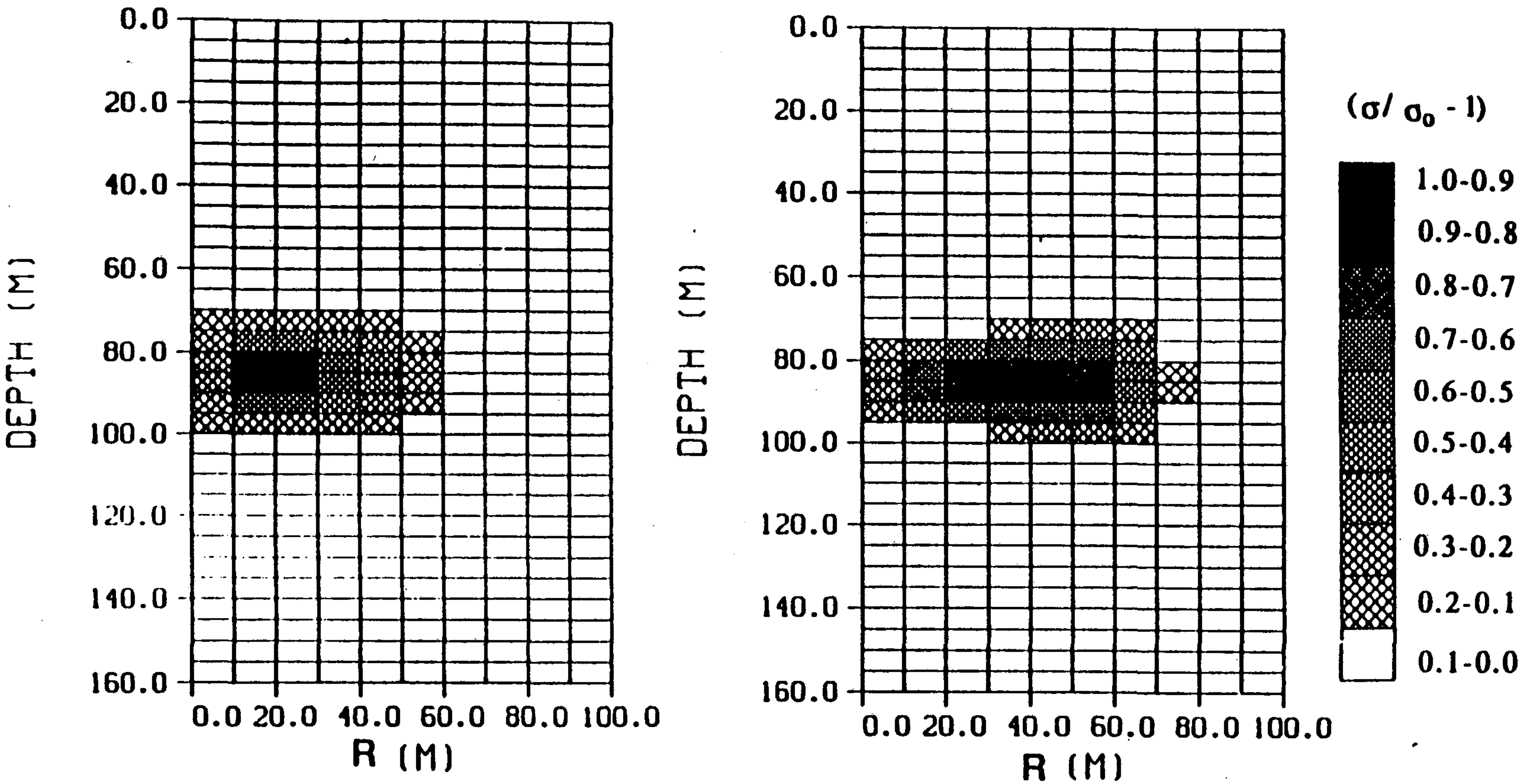

(c) Lx= 40m

(d) Lx= 60m

Figure 1

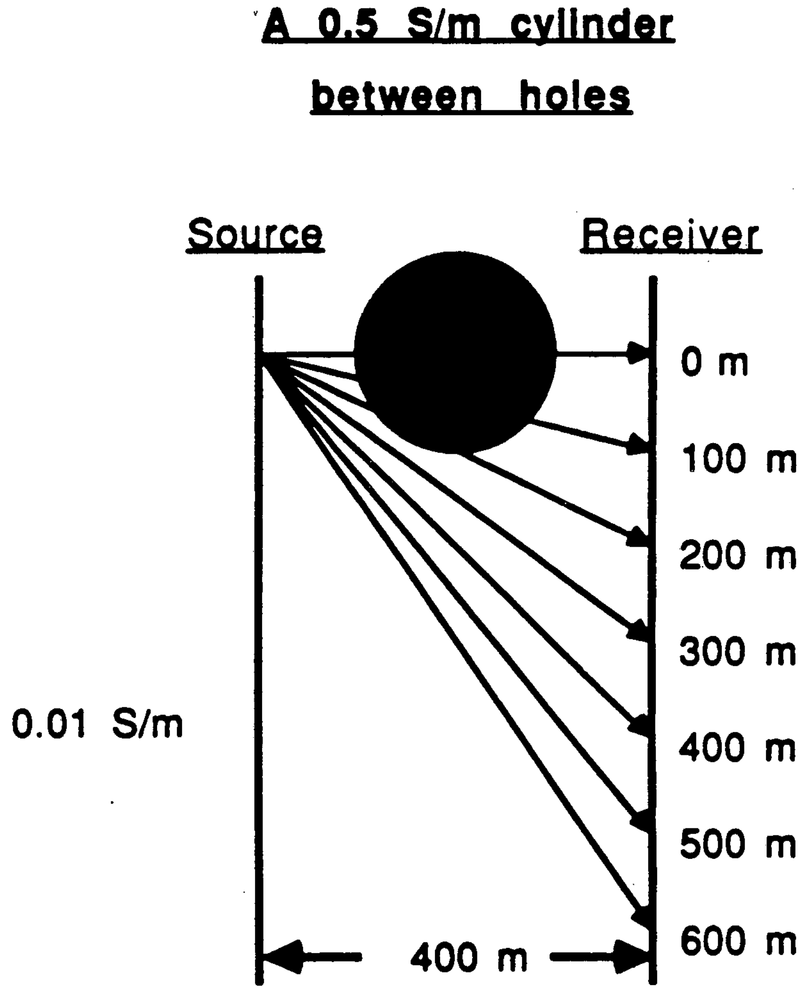
A 0.5 S/m cylinder
between holes
Source
Receiver
0 m
100 m
200 m
300 m
400 m
500 m
600 m
0.01 S/m
400 m

Figure 2

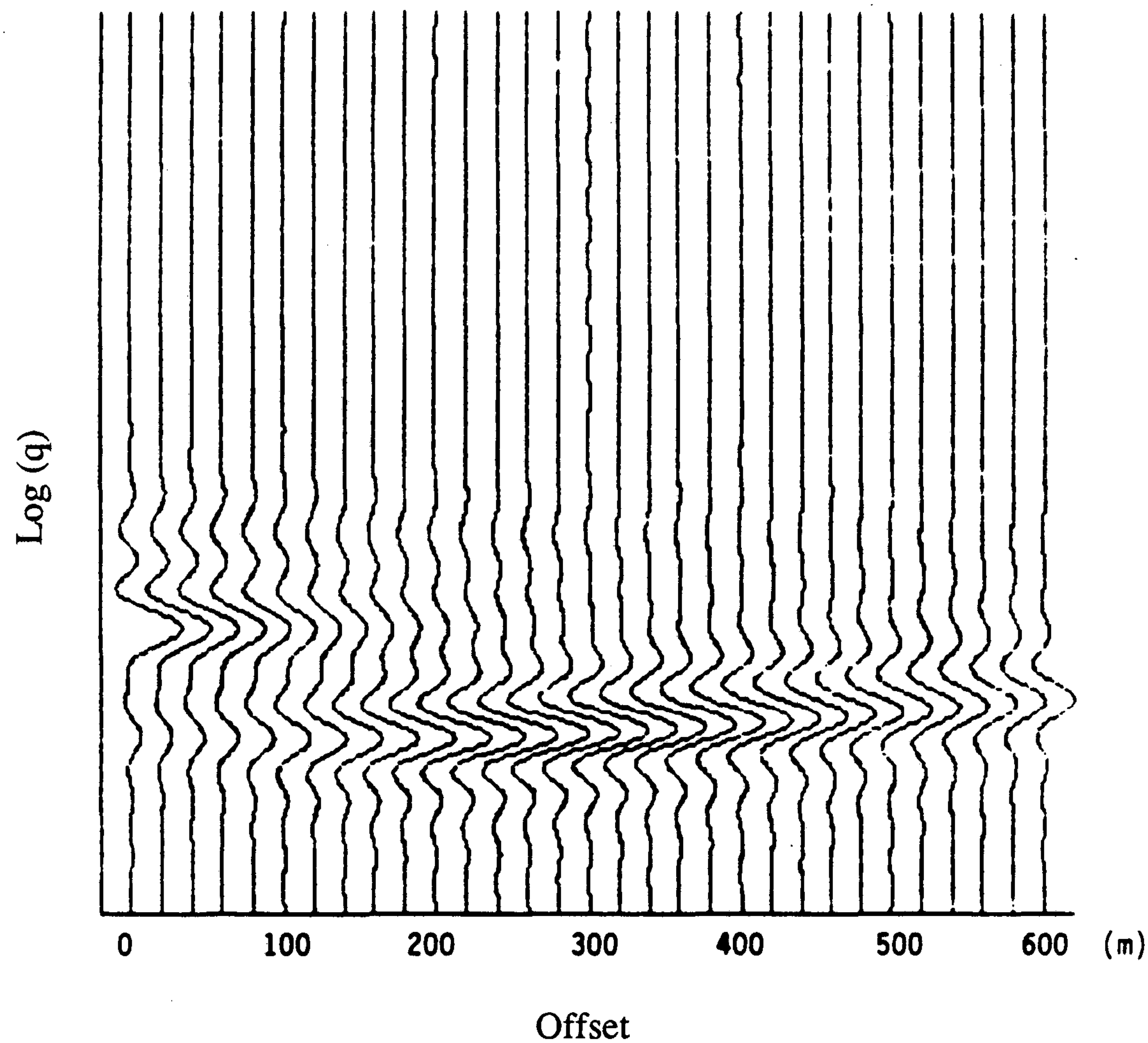

Figure 3

LAWRENCE BERKELEY LABORATORY
UNIVERSITY OF CALIFORNIA
INFORMATION RESOURCES DEPARTMENT
BERKELEY, CALIFORNIA 94720